# Coordination−Addition Polymerization and Kinetic Resolution of Methacrylamides by Chiral Metallocene Catalysts

**Garret Miyake,[†] Lucia Caporaso,[‡] Luigi Cavallo,*[,‡] and Eugene Y.-X. Chen*[,†]**

*Department of Chemistry, Colorado State University, Fort Collins, Colorado 80523-1872, and Dipartimento di Chimica, Università di Salerno, Via Ponte don Melillo, I-84084 Fisciano (SA), Italy*

*Received December 2, 2008; Revised Manuscript Received January 14, 2009*

ABSTRACT: This contribution reports the first successful coordination−addition polymerization of *N,N*-dialkylmethacrylamides and the first example of kinetic resolution of a racemic methacrylamide by chiral metallocene catalysts. The polymerization of methacryloyl-2-methylaziridine (MMAz) by *rac*-(EBI)$Zr^+$-(THF)[OC(O$^i$Pr)=$CMe_2$][$MeB(C_6F_5)_3$]$^-$ (**1**) is stereospecific and also exhibits a high degree of control over polymerization. This polymerization follows first-order kinetics in both concentrations of monomer and catalyst, consistent with a monometallic propagation mechanism involving the fast step of intramolecular conjugate addition within the catalyst−monomer coordination complex leading to the eight-membered-ring resting intermediate. Substituents on the highly strained aziridine ring stabilize the aziridine moiety against thermally induced cross-linking through its ring-opening reaction; thus, the polymer derived from methacryloyl-tetramethyleneaziridine (MTMAz) exhibits greatly enhanced resistance toward thermal cross-linking over poly(MMAz), marking 57 and 42 °C higher onset cross-linking and maximum cross-linking temperatures, respectively. Enantiomeric catalyst (*S,S*)-**1** demonstrates experimentally and theoretically its ability to kinetically resolve the racemic MMAz monomer with a low stereoselectivity factor *s* of 1.8. Polymerizability of several methacrylamide monomers has been investigated via a combined experimental and theoretical (DFT) study that examines the degree of conjugation between the vinyl and carbonyl double bonds, relative polymerization reactivity, and relative energy for the formation of amide−enolate intermediates.

## Introduction

There is increasing interest in the utilization of technologically important, single-site cationic group 4 metallocene catalysts,[1] which have been extensively investigated and successfully employed for the (co)polymerization of nonpolar vinyl monomers (α-olefins in particular),[2] for polymerizations of polar, functionalized vinyl monomers including methacrylates,[3−45] acrylates,[40,46−49] acrylamides,[50−53] and methyl vinyl ketone.[54] The polymerization of (meth)acrylates has also been studied computationally.[55−62] Certain catalyst structures exhibit a high degree of control over polymerization characteristics (activity and efficiency; polymer molecular weight, MW; MW distribution, MWD; livingness) and stereochemistry (polymer tacticity and stereocontrol mechanism), enabling the ambient-temperature synthesis of highly isotactic poly(methacrylate)s (≥95% *mm*)[8,12,35,43,44] and poly(acrylamide)s (>99% *mm*)[50−53] using chiral $C_2$-ligated zirconocenium complexes as well as highly syndiotactic poly(methacrylate)s (≥94% *rr*)[3] using chiral $C_s$-ligated zirconocenium complexes. An important *exception* here is the inability of such coordination metallocene catalysts to polymerize *N,N*-dialkylmethacrylamides such as *N,N*-dimethylmethacrylamide (DMMA),[52] although they can polymerize acrylamides such as *N,N*-dimethylacrylamide (DMAA) rapidly in a stereospecific and living fashion.[50−53]

The nonpolymerizability of DMMA has also been previously noted in anionic polymerizations by organolithium initiators,[63] which was attributed to a twisted, nonconjugated monomer conformation between the vinyl and carbonyl double bonds, caused by steric repulsions between the α-methyl group or the vinyl proton and the *N*-methyl group of DMMA. As compared to other polymerizable conjugated monomers such as DMAA, this twisted DMMA monomer conformation results in a less effective π overlap between these two functional groups and thus leads to unstable amide enolate intermediates upon nucleophilic attack by the initiator. This hypothesis was supported by MNDO calculations[63] and NMR studies;[64] the calculations reveal an energy minimum for the twisted confirmation that lies ∼4.0 kcal/mol below either the *s-cis* or *s-trans* conformation, while the $^1$H and $^{13}$C NMR studies show that the NMR features (chemical shifts and peak separations) for the vinyl protons and carbonyl carbons of the nonpolymerizable *N,N*-dialkylmethacrylamides more closely resemble those of nonconjugated vinyl monomers than those of polymerizable, conjugated monomers. Introduction of the highly strained, three-membered aziridine ring into the monomer structure provided a clever solution to the nonpolymerizability of *N,N*-dialkylmethacrylamides; Okamoto and Yuki[65] reported in 1981 successful anionic and radical polymerizations of *N*-methacryloylaziridine with $^n$BuLi or PhMgBr at −78 °C and with AIBN, and most recently Ishizone and co-workers[66] reported living anionic polymerization of *N*-methacryloyl-2-methylaziridine (MMAz) with 1,1-diphenyl-3-methylpentyllithium or diphenylmethylpotassium in the presence of LiCl or $Et_2Zn$ at low temperatures (−40 to −78 °C).

Three unique features about MMAz and its analogous methacrylamide monomers can be appreciated. First, based on our DFT calculations (vide infra), linking the two *N*-alkyl groups into a small three-membered ring alleviates the nonbonding interaction incurred to DMMA, giving rise to the desired planar, *s-cis* (C=C/C=O) conjugated conformation for MMAz and thereby solving the nonpolymerizability issue with *N,N*-dialkylmethacrylamides. Second, the pendant strained aziridine ring provides needed reactivity toward further polymer functionalization or chain cross-linking, through its ring-opening reactions, for stable polymer network structures.[66] Third, MMAz is a racemic monomer, which can be tested for kinetic resolution polymerization, with appropriate enantiomeric catalysts, potentially leading to the enantiomeric monomer with appreciable % *ee* and the optically active polymer which predominately incorporates the other enantiomer from the racemic monomer

* Corresponding authors. E-mail: lcavallo@unisa.it (L.C.); eugene.chen@colostate.edu (E.Y.-X.C.).
[†] Colorado State University.
[‡] Università di Salerno.

10.1021/ma802697z CCC: $40.75 
Published on Web 02/13/2009

**Chart 1. Chemical Structures of the Catalysts Employed and the Monomers Investigated in This Study**

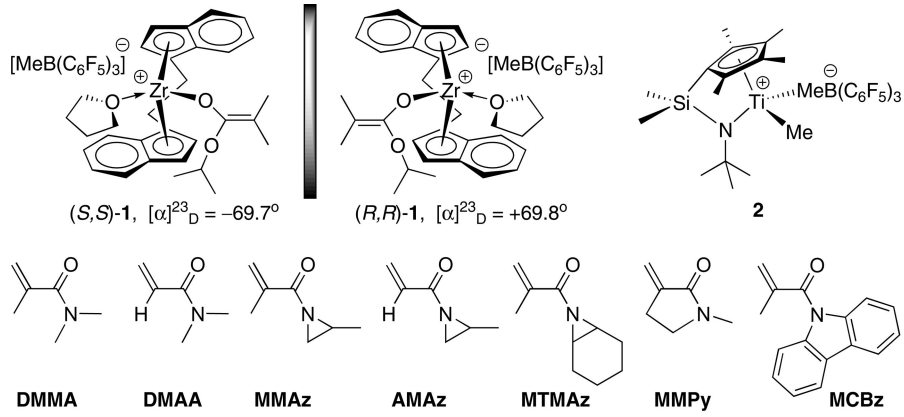


pool. These three reasoned unique features about MMAz prompted our current research using chiral metallocene catalysts, including $C_2$-ligated ester enolate complex *rac*-(EBI)$Zr^+$-(THF)[OC(O$^i$Pr)═$CMe_2$][$MeB(C_6F_5)_3$]$^-$ [**1**; EBI = $C_2H_4(\eta^5$-indenyl)$_2$][8,12,52] and $C_s$-ligated alkyl complex (CGC)$TiMe^+$MeB-$(C_6F_5)_3^-$ [**2**; CGC = $Me_2Si(\eta^5$-$C_5Me_4)$($^t$BuN)],[17,55] as we have previously demonstrated their remarkable ability to precisely control the polymerization of methacrylates and acrylamides and also to render asymmetric, living polymerization when enantiomeric catalysts **1** are employed.[50,51] Accordingly, this study was designed to address the following four fundamental questions: (1) Can such coordination metallocene catalysts, which have been shown not to polymerize nonconjugated methacrylamides such as DMMA,[52] polymerize conjugated methacrylamides such as MMAz? (2) If the answer to the polymerizability question is positive, then is the polymerization well-controlled and can the enantiomeric catalysts effect kinetic resolution of the racemic MMAz monomer? (3) Can we design other conjugated methacrylamide monomers with effective vinyl and carbonyl $\pi$ overlap and thus good polymerizability, thereby allowing for a study of the polymer structure−property (e.g., thermal stability) relationship? (4) What determines polymerizability of methacrylamides? Chart 1 summarizes the catalysts employed and the scope of the methacrylamide monomers investigated in this study toward addressing the above four fundamental questions.

## Experimental Section

**Materials and Methods.** All syntheses and manipulations of air- and moisture-sensitive materials were carried out in flamed Schlenk-type glassware on a dual-manifold Schlenk line, a high-vacuum line, or in an argon or nitrogen-filled glovebox. HPLC-grade organic solvents were sparged extensively with nitrogen during filling of the solvent reservoir and then dried by passage through activated alumina (for $Et_2O$, THF, and $CH_2Cl_2$) followed by passage through Q-5-supported copper catalyst (for toluene and hexanes) stainless steel columns. Benzene, benzene-$d_6$, and toluene-$d_8$ were degassed, dried over sodium/potassium alloy, and vacuum-distilled or filtered, whereas $C_6D_5Br$, $CDCl_3$, and $CD_2Cl_2$ were dried over activated Davison 4 Å molecular sieves. NMR spectra were recorded on either a Varian Inova 300 (FT 300 MHz, $^1$H; 75 MHz, $^{13}$C; 282 MHz, $^{19}$F) or a Varian Inova 400 spectrometer. Chemical shifts for $^1$H and $^{13}$C spectra were referenced to internal solvent resonances and are reported as parts per million relative to tetramethylsilane, whereas $^{19}$F NMR spectra were referenced to external $CFCl_3$. High-resolution mass spectrometry (HRMS) data were collected using Agilent 6220 accurate time-of-flight LC/MS spectrometer.

Cyclohexene oxide, 2-methylaziridine, $^n$BuLi (1.6 M in hexanes), indene, 1,2-dibromoethane, tetrachlorozirconium, triflic acid, lithium dimethylamide, diisopropylamine, sodium azide, sodium hydride, 1,1,3,3-tetramethylguanidine, (2*S*,4*S*)-pentanediol (99% *ee*, $[\alpha]^{20}_D$ +39.8 ($c$ = 10, $CHCl_3$), (2*R*,4*R*)-pentanediol (97% *ee*, $[\alpha]^{21}_D$ −40.4 ($c$ = 10, $CHCl_3$), $(CF_3SO_2)_2O$, $BPhCl_2$, MeMgI (3.0 M in diethyl ether), 1,2-dibromobenzene, and trifluoroacetic acid were purchased from Aldrich. Methacryloyl chloride, acryloyl chloride, triethylamine, *N,N*-dimethylaniline, *N*-methylpyrrolidone, diethyl oxalate, carbazole, and 2,6-dimethylpyridine were purchased from Alfa Aesar. Trimethylaluminum (neat) was purchased from Strem Chemical Co., and isopropyl isobutyrate was purchased from TCI America. All commercial reagents were used as received unless indicated as follows. Cyclohexene oxide, indene, 1,2-dibromoethane, 1,2-dibromobenzene, *N,N*-dimethylaniline, methacryloyl chloride, and acryloyl chloride were degassed using three freeze−pump−thaw cycles, while 2-methylaziridine, diisopropylamine, diethyl oxalate, $(CF_3SO_2)_2O$, and $BPhCl_2$ were vacuum-distilled. The reagents 2,6-dimethylpyridine, triethylamine, and isopropyl isobutyrate were degassed and dried over $CaH_2$ overnight, followed by vacuum distillation. 1,4-Dioxane (Fisher) was degassed, dried over sodium/potassium alloy, and vacuum-distilled.

Tris(pentafluorophenyl)borane, $B(C_6F_5)_3$, was obtained as a research gift from Boulder Scientific Co. and further purified by recrystallization from hexanes at −35 °C inside a glovebox. The $(C_6F_5)_3B\cdot$THF adduct was prepared by addition of THF to a toluene solution of the borane followed by removal of the volatiles and drying in vacuo. Literature procedures were employed for the preparation of the following compounds and metallocene complexes: cyclohexenime,[67] LiOC(O$^i$Pr)═$CMe_2$,[55] (EBI)$H_2$,[68] *rac*-(EBI)$Zr(NMe_2)_2$,[69] *rac*-(EBI)$ZrMe_2$,[69] *rac*-(EBI)ZrMe(OTf),[12] *rac*-(EBI)ZrMe[OC(O$^i$Pr)═$CMe_2$],[12] *rac*-(EBI)$Zr^+$(THF)[OC(O$^i$Pr)═$CMe_2$][$MeB(C_6F_5)_3$]$^-$ (**1**),[12] (*R,R*)- and (*S,S*)-(EBI)$ZrCl_2$,[70] (*R,R*)- and (*S,S*)-(EBI)$ZrMe_2$,[50,51] (*R,R*)- and (*S,S*)-(EBI)ZrMe(OTf),[50,51] (*R,R*)- and (*S,S*)-(EBI)ZrMe[OC(O$^i$Pr)═$CMe_2$],[50,51] (*R,R*)- and (*S,S*)-**1**,[50,51] (CGC)$TiMe_2$,[71] and CGC$TiMe^+$MeB$(C_6F_5)_3^-$ (**2**).[72]

**Monomer Preparations.** Literature procedures were employed to prepare monomers methacryloyl-2-methylaziridine (MMAz),[66] acryloyl-2-methylaziridine (AMAz),[66] and α-methylene-*N*-methylpyrrolidone (MMPy).[73] Methacryloyl cyclohexenimine or methacryloyl tetramethyleneaziridine (MTMAz) was prepared by reacting cyclohexenimine with methacryloyl chloride in the presence of triethylamine. Specifically, a 200 mL Schlenk flask was loaded with cyclohexenimine (2.40 g, 24.7 mmol), triethylamine (2.49 g, 24.7 mmol), and $CH_2Cl_2$ (50 mL) and then capped with a septum. The solution of the mixture was cooled to 0 °C under positive $N_2$ flow before the dropwise addition of methacryloyl chloride (2.58 g, 24.7 mmol) via syringe. The reaction mixture was gradually warmed to room temperature, while being stirred for 15 h, after which the volatiles were removed in vacuo, affording a white solid. $Et_2O$ (100 mL) was added to the solid, and the resulting suspension was filtered through a medium porosity glass frit. The solvent of the filtrate was removed via roto-vap, and the residual monomer was purified by distillation, drying over $CaH_2$ overnight, and vacuum distillation (bp = 52−54 °C, 1 atm), affording 1.66 g

(40.7%) of MTMAz as a colorless oil. $^1$H NMR ($CDCl_3$, 23 °C): $\delta$ 5.99 and 5.55 (s, 2H, $CH_2$=), 2.61−2.59 (m, 2H, CH), 1.97−1.78 (m, 4H, $CH_2$), 1.90 (s, 3H, $CH_3$), 1.49−1.36 (m, 2H, $CH_2$), 1.19−1.17 (m, 2H, $CH_2$). $^{13}$C NMR ($CDCl_3$, 23 °C): $\delta$ 180.9 (*C*=O), 139.5 (*C*=$CH_2$), 128.8 (*C*=*C*$H_2$), 36.39 (N*C*$HCH_2$), 23.65 ($CHCH_2CH_2$), 19.74 ($CHCH_2CH_2$), 18.38 (C*Me*). HRMS (APCI): *m*/*z* calcd for $C_{10}H_{16}NO$: $[M + H]^+$: 166.12264; found: 166.12296.

MCBz was prepared by reacting carbazole with methacryloyl chloride in THF in the presence of triethylamine. Specifically, a 500 mL Schlenk flask was loaded with carbazole (10.8 g, 64.6 mmol), triethylamine (6.54 g, 64.60 mmol), and 200 mL of THF. The solution was cooled to 0 °C under positive $N_2$ flow before the dropwise addition of methacryloyl chloride (6.75 g, 64.59 mmol). The reaction mixture was gradually warmed to room temperature while being stirred for 24 h, after which the suspension was filtered through a medium porosity glass frit, the solvent of the filtrate was removed via roto-vap, and the resulting product was purified by three recrystallizations from a toluene/hexanes solution mixture, affording a white solid (1.67 g, 10.9%) of MCBz. $^1$H NMR ($CDCl_3$, 23 °C): $\delta$ 8.14 (d, $J$ = 6.3 Hz, 2H, Ar), 8.01 (d, $J$ = 5.7 Hz, 2H, Ar), 7.49−7.37 (m, 4H, Ar), 5.69 and 5.63 (s, 2H, $CH_2$=), 2.26 (s, 3H, $CH_3$). $^{13}$C NMR ($CDCl_3$, 23 °C): $\delta$ 170.6 (*C*=O), 141.5 (*C*=$CH_2$), 138.4 (N*C*CH, Ar), 125.9 (C*C*CH, Ar), 122.4 (*C*=*C*$H_2$), 126.8, 123.4, 119.7, and 115.8 (Ar), 19.24 (C*Me*). HRMS (APCI): *m*/*z* calcd for $C_{16}H_{14}NO$: $[M + H]^+$: 236.10699; found: 236.10699.

**General Polymerization Procedures.** Polymerizations were performed in 30 mL oven-dried glass reactors inside the glovebox. In a typical polymerization procedure at ambient temperature, predetermined amounts of $B(C_6F_5)_3$·THF and the appropriate precatalyst were premixed in 10 mL of $CH_2Cl_2$ (for AMAz polymerizations) or 2 mL of $CH_2Cl_2$ (for MMAz and MTMAz polymerizations). For polymerizations with the (CGC)$TiMe_2$ precatalyst at 60 °C, (CGC)$TiMe_2$ (7.80 mg, 23.8 $\mu$mol), $B(C_6F_5)_3$ (12.2 mg, 23.8 $\mu$mol), and 2 mL of 1,2-dichlorobenzene were added to a 25 mL Schlenk flask, which was capped with a septum. The flask was brought out of the box and connected to a Schlenk line and heated to 60 °C. After 10 min, the monomer (AMAz, 3.2 mmol; MMAz, 3.2 mmol; MTMAz, 1.5 mmol) was added via syringe and allowed to stir for a predetermined time interval. Polymerizations were stopped by pouring the solutions into a 10-fold excess of $Et_2O$, and polymers were isolated by filtration or centrifugation, washed with $Et_2O$, and dried in vacuo at ambient temperature.

**Kinetics of MMAz Polymerization.** Kinetic experiments for the polymerization of MMAz were carried out in 30 mL reactors inside of the glovebox at room temperature using a similar procedure as already described above, except that, at appropriate time intervals, 0.1 mL aliquots were withdrawn from the reaction mixture using a syringe and quickly quenched into 1 mL septum-cap-sealed vials containing 0.6 mL of undried "wet" $CDCl_3$ mixed with 250 ppm of BHT-H. The quenched aliquots were analyzed by $^1$H NMR for monomer conversion. The monomer conversion of MMAz at time $t$ was determined by comparing the methyl singlet centered at 1.95 ppm of the unreacted monomer to the methyl peaks on the aziridine ring (monomer and polymer) and the methyl peak from the polymer main chain, which are centered at 1.30 ppm. Specifically, percent monomer conversion was calculated by the formula $(A_{1.30} - A_{1.95})/(A_{1.30} + A_{1.95}) \times 100$, where $A_{1.30}$ is the total integral for the peaks centered at 1.30 ppm and $A_{1.95}$ is the total integral for the peak centered at 1.95 ppm.

**Kinetic Resolution of (Meth)acryloyl-2-methylaziridines.** The kinetic resolution of (meth)acryloyl-2-methylaziridines was carried out in 30 mL reactors inside of the glovebox at ambient temperature using a similar procedure as already described above, except employing the enantiomeric catalyst (*S,S*)-**1**. At predetermined time intervals 0.1 mL (MMAz) or 0.2 mL (AMAz) aliquots were withdrawn from the polymerization reaction using a syringe and quickly quenched into 1 mL septum cap sealed vials containing 0.6 mL of undried "wet" $CDCl_3$ mixed with 250 ppm of BHT-H. The quenched aliquots were analyzed by $^1$H NMR for monomer conversion. The aliquots were then filtered through a silica column to completely remove polymer and catalyst residues, as confirmed by $^1$H NMR and HPLC. The solvent was removed via roto-vap and the % *ee* of the monomer was measured using an Agilent 1100 Series HPLC with a flow rate of 1.0 mL/min. MMAz was analyzed with a Chiracel OB-H column at 25 °C (80:20 hexanes:$^i$PrOH, 1.0 mL/min, major enantiomer: 6.4 min, minor enantiomer: 7.8 min). AMAz was analyzed with a Chiracel AS-H column at 25 °C (97:3 hexanes:$^i$PrOH, 1.0 mL/min, major enantiomer: 11.2 min, minor enantiomer 10.4 min).

**Polymer Characterizations.** Gel permeation chromatography (GPC) and light scattering (LS) analyses of the polymers were carried out at 40 °C and a flow rate of 1.0 mL/min, with DMF (for PMMAz samples produced by **1**) or $CHCl_3$ (for all other samples) as the eluent, on a Waters University 1500 GPC instrument equipped with four 5 $\mu$m PL gel columns (Polymer Laboratories) and Wyatt miniDAWN TREOS multiangle (45°, 90°, 135°) light scattering detector. LS data were processed with Wyatt Astra Software (version 5.3.2.15), and d$n$/d$c$ values were determined assuming 100% mass recovery of polymers with known concentrations.

Maximum rate decomposition temperatures ($T_{max}$) and decomposition onset temperatures ($T_{onset}$) of the polymers were measured by thermal gravimetric analysis (TGA) on a TGA 2950 thermogravimetric analyzer, TA Instruments. Polymer samples were heated from ambient temperature to 600 °C at a rate of 20 °C/min. Values for $T_{max}$ were obtained from derivative (wt %/°C) versus temperature (°C) plots while $T_{onset}$ and $T_{end}$ values (initial and end temperatures) were obtained from wt % versus temperature (°C) plots. Glass transition temperatures ($T_g$) and cross-linking temperatures ($T_c$) of the polymers were measured by differential scanning calorimetry (DSC) on a DSC 2920, TA Instruments.

**Computational Details.** The Amsterdam Density Functional (ADF) program[74] was used to obtain all the results discussed in this work. The electronic configuration of the molecular systems was described by a triple-$\zeta$ STO basis set on Zr (ADF basis set TZV).[74a] A triple-$\zeta$ STO basis set, augmented by one polarization function, was used for main group atoms (ADF basis sets TZVP).[74a] The inner shells on Zr (including 3d), C, N, and O (1s) were treated within the frozen core approximation. Energies and geometries were evaluated using the local exchange-correlation potential by Vosko et al.,[75] augmented in a self-consistent manner with Becke's[76] exchange gradient correction and Perdew's[77] correlation gradient correction (BP86 functional). All geometries were localized in the gas phase. However, since methacrylamide polymerization is usually performed in a rather polar solvent, such as $CH_2Cl_2$, we performed single-point energy calculations on the final geometries to take into account solvent effects. The ADF implementation of the conductor-like screening model (COSMO)[78] was used. A dielectric constant of 8.9 and a solvent radius of 2.94 Å were used to represent $CH_2Cl_2$ as the solvent. The following radii, in angstroms, were used for the atoms: H 1.16, C 2.00, N 1.40, O 1.50, and Zr 2.40. All the reported energies include solvent effects.

## Results and Discussion

**Polymerization of Methacrylamide MMAz.** We have previously reported that the living/controlled polymerization of *N,N*-dialkyl- and *N,N*-diarylacrylamides by catalyst **1** proceeds via a monometallic, site-controlled, coordination (conjugated)−addition mechanism through eight-membered-ring amide enolate intermediates (Scheme 1).[50,52] The resting state during a propagation "catalysis" cycle is the cyclic amide enolate, and associative displacement of the coordinated penultimate amide group by incoming acrylamide monomer to regenerate the catalyst−monomer complex is the rate-determining step, giving rise to the propagation kinetics that is first order in both concentrations of the monomer and the catalyst. We also noted that the methacrylamide DMMA is not polymerized by such metallocene catalysts.[52]

As a control to examine whether the reactive aziridine ring incorporated in the predictably polymerizable MMAz would remain intact under our metallocene polymerization conditions

**Scheme 1. Initiation and Propagation Steps Involved in the Polymerization of Acrylamides by *rac*-1**

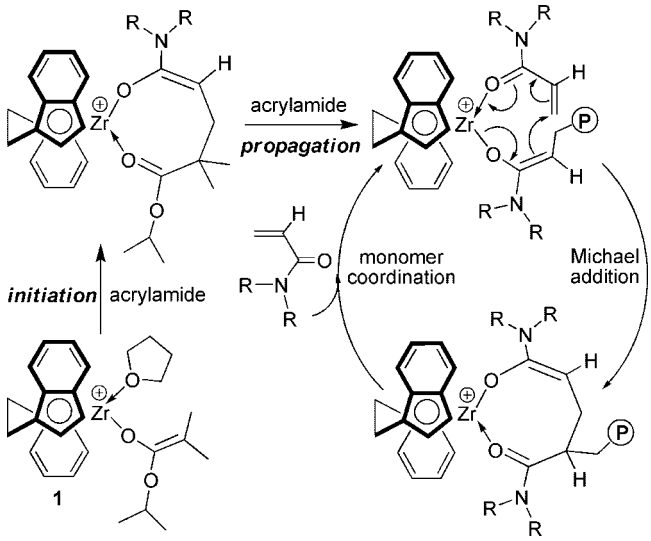


**Table 1. Results of Polymerization of (Meth)acrylamides by 1 at Ambient Temperature[a]**

| run no. | monomer | [M]/[**1**] | time (min) | conv[b] (%) | $M_w$[c] (kg/mol) | PDI[c] ($M_w/M_n$) | $I$*[d] (%) |
|---|---|---|---|---|---|---|---|
| 1 | AMAz | 100 | <1 | 100 | 13.1 | 1.02 | 87 |
| 2 | MMAz | 100 | 60 | 85.3 | 12.3 | 1.01 | 89 |
| 3 | MMAz | 200 | 60 | 81.3 | 22.3 | <1.01 | 92 |
| 4 | MMAz | 400 | 60 | 83.9 | 80.9 | <1.01 | 52 |
| 5 | MTMAz | 100 | 60 | 93.9 | 25.1 | 1.02 | 65 |

[a] Carried out in 10 mL (for AMAz) or in 2 mL (for MMAz and MTMAz) of $CH_2Cl_2$ at ambient temperature (~23 °C). [b] Monomer conversion measured by $^1$H NMR. [c] Determined by light scattering. [d] Initiator efficiency $I^* = M_n(\text{calcd})/M_n(\text{exptl})$, where $M_n(\text{calcd}) = \text{MW(M)} \times [\text{M}]/[\mathbf{1}] \times \text{conversion (\%)} + \text{MW of chain-end groups}$.

or not, we first investigated the polymerization of the acrylamide AMAz (which also adopts a stable conjugated *s-cis* conformation as predicted by DFT) with chiral, racemic catalyst **1** in $CH_2Cl_2$ at room temperature. The polymerization of 100 equiv of AMAz by 1 equiv of **1** is rapid, achieving quantitative monomer conversion in <1 min; it proceeds exclusively via C−C bond formation, as shown by the disappearance of the monomer vinyl protons, while leaving the aziridine ring intact, as confirmed by $^1$H NMR of the resulting polymer. The polymer obtained has a $M_w$ of 13.1 kg/mol (by LS detector) with a narrow MWD of 1.02 (run 1, Table 1), giving an initiator efficiency ($I$*) of 87%. Hence, the polymerization of AMAz is fast, efficient, and controlled, and it involves no ring-opening of the aziridine ring under the current conditions.

Having established the inertness of the aziridine ring toward the metallocene polymerization conditions, we subsequently investigated the polymerization of the methacrylamide MMAz by **1**. Gratifyingly, like the polymerization of AMAz, the polymerization of MMAz by **1** is effective and controlled (runs 2−4 vs run 1, Table 1), although the latter polymerization is considerably slower even with a 5-fold increased concentration and did not achieve a high initiator efficiency at a higher [M]/[**1**] ratio of 400. Nonetheless, the MMAz polymerization by **1** exhibits a high degree of control in [M]/[**1**] ratios of ≤200, producing the well-defined polymer without ring-opening of the aziridine moiety within the MMAz repeat unit. As expected, this polymerization by the isospecific catalyst **1** yields the highly isotactic polymer *with no detectable stereodefects*, as shown by the $^{13}$C NMR spectrum of the polymer (Figure 1).

Monitoring of the MMAz polymerization by **1** in a [M]/[**1**] ratio of 100 reveals a first-order dependence on [MMAz], a linear increase in MW with monomer conversion, and narrow

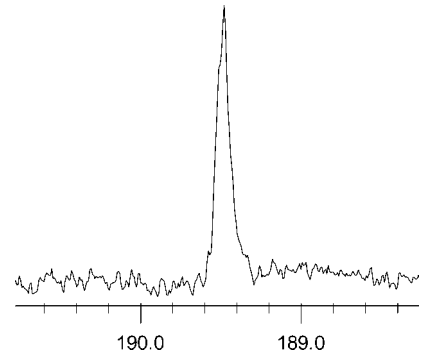


**Figure 1.** $^{13}$C NMR showing the C=O region of the highly isotactic poly(MMAz) (run 4, Table 1) in $CDCl_3$ at 60 °C.

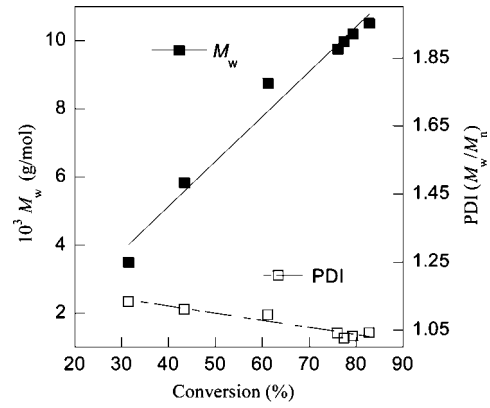


**Figure 2.** Plots of $M_w$ (by LS) and PDI of poly(MMAz) versus MMAz conversion in $CH_2Cl_2$ at ambient temperature (~23 °C): [MMAz] = 1.59 M, [*rac*-**1**] = 15.9 mM.

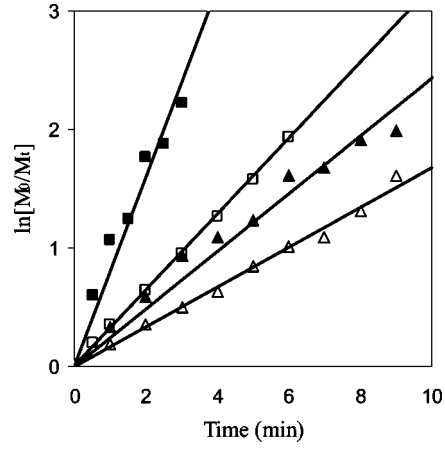


**Figure 3.** Semilogarithmic plots of $\ln([\text{MMAz}]_0/[\text{MMAz}]_t)$ vs time for the polymerization of MMAz by **1** in $CH_2Cl_2$ at ambient temperature (~23 °C). Conditions: $[\text{MMAz}]_0 = 1.59$ M; $[\mathbf{1}]_0 = 15.9$ mM (■), 7.99 mM (□), 5.33 mM (▲), and 3.99 mM (Δ).

MWDs ranging from 1.14 to 1.01 (Figure 2). Kinetic experiments employed the $[\text{MMAz}]_0/[\mathbf{1}]_0$ ratios ranging from 100 to 400, showing the first-order dependence on [MMAz] for the ratios (Figure 3). Furthermore, a double-logarithm plot (Figure 4) of the apparent rate constants ($k_{app}$), obtained from the slopes of the best-fit lines to the plots of $\ln([\text{MMAz}]_0/[\mathbf{1}]_0)$ vs time as a function of $\ln[\mathbf{1}]_0$, was fit to a straight line ($R^2 = 0.99$) with a slope of 1.12. Thus, the kinetic order with respect to [**1**], given by the slope of ~1, reveals that the propagation is also first order in catalyst concentration, indicating that the polymerization of MMAz by catalyst **1** follows the same coordination−addition

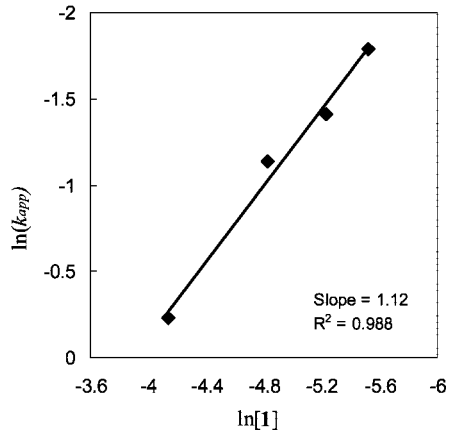


**Figure 4.** Plot of ln($k_{app}$) vs ln[**1**] for the MMAz polymerization by **1** in $CH_2Cl_2$ at ambient temperature (~23 °C).

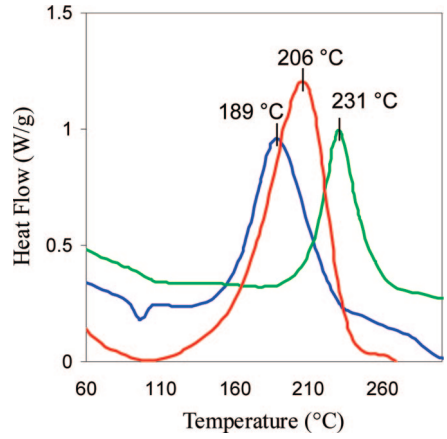


**Figure 5.** DSC plots of poly(MMAz) (blue), poly(AMAz) (red), and poly(MTMAz) (green) acquired at a scanning rate of 10 °C/min.

mechanism as that of the acrylamide polymerization shown in Scheme 1.

We also examined the MMAz polymerization using the $C_s$-ligated titanium alkyl complex **2**. The polymerization of 200 equiv of MMAz by 1 equiv of **2** in $CH_2Cl_2$ is sluggish at ambient temperature, achieving only 62.6% monomer conversion in 27 h. The polymer produced exhibits a narrow MWD of 1.17, but its measured $M_w$ of 108 kg/mol (by LS) is much larger than the calculated according to the monomer to catalyst feed ratio of 200. The rate of this polymerization is significantly enhanced when carried out at 60 °C in 1,2-dichlorobenzene, achieving similar conversion (64.7%) in just 5 h. Again, the measured $M_w$ of 104 kg/mol for the resulting polymer is considerably higher than the calculated, and the polymer produced at this elevated temperature also has a broader MWD of 1.38. The much higher MWs of these polymers afforded by **2** are presumably related to slow initiation by the titanium−alkyl ligand in **2**, as compared to propagation by the titanium−amide enolate ligand, while the broader MWD of the polymer produced at elevated temperature may be contributed to side reactions such as noncoordination pathways (i.e., radical polymerization) known for acrylamide polymerization by metallocene alkyl complexes[53] and partial ring-opening of the aziridine ring. The syndiotacticity of the poly(MMAz) cannot be accurately determined by $^{13}C$ NMR due to the overlapping of the *mr* and *rr* triad peaks in the C═O region.

**Thermal Properties of Methacrylamide Polymers Incorporating the Aziridine Ring.** We reasoned that substituents on the highly strained aziridine ring should sterically protect it against ring-opening, thus making it less susceptible to thermally induced cross-linking. To this end, we synthesized an additional methacrylamide polymer, poly(MTMAz) with cyclic tetramethylene substitution, for a comparative study. The MTMAz monomer (Chart 1) was readily polymerized by **1** at ambient temperature in a [M]/[**1**] ratio of 100, achieving 94% monomer conversion in 1 h. The poly(MTMAz) obtained has a $M_w$ of 25.1 kg/mol and a narrow MWD of 1.02 (run 5, Table 1). This polymer, together with poly(AMAz) and poly(MMAz)s produced by **1**, was analyzed by TGA and DSC.

TGA results showed that the methacrylamide polymers are more resistant to thermal degradation than the acrylamide derivative. Specifically, poly(MMAz) and poly(MTMAz) exhibit $T_{onset}$ (initial) at 406 °C ($T_{max}$ = 443 °C) and 391 °C ($T_{max}$ = 435 °C), respectively, while poly(AMAz) has a $T_{onset}$ at a much lower temperature of 337 °C ($T_{max}$ = 419 °C). Interestingly, although all three polymers decomposed in a single decomposition process, the decomposition window for poly(AMAz) is much larger than either poly(MMAz) or poly(MTMAz). Thus, poly(AMAz) exhibits a $T_{end}$ of 453 °C, while poly(MMAz) and poly(MTMAz) show $T_{end}$ of 464 and 446 °C, respectively.

DSC analyses determined a higher $T_g$ of 92.9 °C for poly(MMAz), as compared to a $T_g$ of 57.7 °C for poly(AMAz); no noticeable glass transition was observable for poly(MTMAz). We also utilized DSC (Figure 5) to monitor the temperature ($T_c$, c for curing or cross-linking) required for inducing thermal cross-linking of the polymers through ring-opening of the aziridine ring.[66] The onset temperature for cross-linking of poly(AMAz) (118 °C) is lower than that of poly(MMAz (143 °C), but interestingly, the temperature for maximum cross-linking of poly(AMAz) (206 °C) is higher than that of poly(MMAz) (189 °C), again reflecting a broad curing temperature window for poly(AMAz). Most significantly, poly(MTMAz) has a high onset $T_c$ of 199 °C and maximum $T_c$ of 231 °C, corresponding to the thermal enhancements of 57 and 42 °C in $T_c$ indices as compared to poly(MMAz).

**Kinetic Resolution of Methacrylamide MMAz.** The above-described success in the living/controlled polymerization of racemic AMAz and MMAz by the racemic catalyst **1** provided a strong basis for our investigation into the potential capability of the enantiomeric metallocene catalyst to discriminate between two enantiomers of the chiral methacrylamide monomer. Scheme 2 outlines the strategy of using enantiomeric catalyst (*S,S*)-**1** to preferentially polymerize one enantiomer from the racemic MMAz poor under ≤50% conversion, thus producing the chiral polymer enriched with this enantiomer while leaving

**Scheme 2. Proposed Kinetic Resolution Polymerization of Racemic MMAz by Enantiomeric (*S,S*)-1**

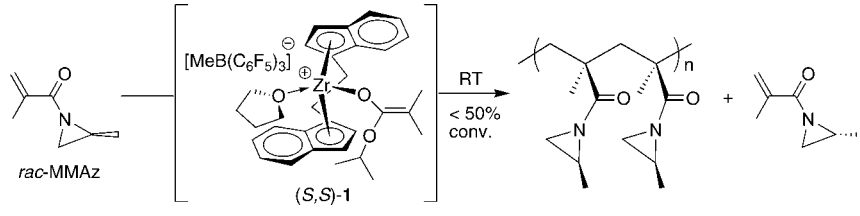

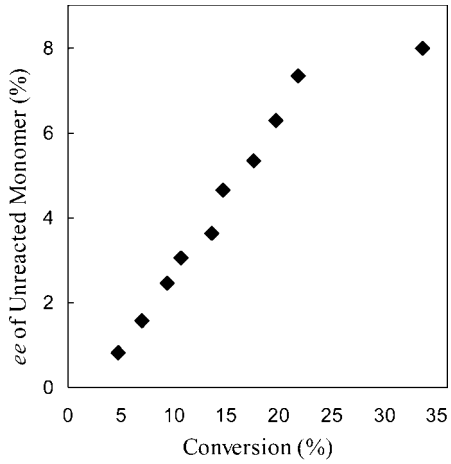


**Figure 6.** Plot of % *ee* of the unreacted MMAz vs % monomer conversion for the kinetic resolution of MMAz by enantiomeric catalyst (*S,S*)**-1** at ambient temperature.

**Table 2. Relative Energies of Four Transition States for the Polymerization of MMAz by (*S,S*)-1**

| transition state | *E* (kcal/mol) |
|---|---|
| *S*-chain/*S*-MMAz | 0.0 |
| *S*-chain/*R*-MMAz | 0.2 |
| *R*-chain/*R*-MMAz | 1.1 |
| *R*-chain/*S*-MMAz | 0.7 |

the other enantiomer enriched in the unreacted monomer. To follow this reasoning, we first examined kinetic resolution of AMAz using enantiomeric (*S,S*)**-1** at ambient temperature by taking an aliquot of the polymerization at a monomer conversion of 53.5%. The unreacted monomer (after complete removal of the polymer and the catalyst residue) was then analyzed by chiral HPLC and found to have a low *ee* of 8.8%, giving a low stereoselectivity factor, or *s* value,[79] of 1.2. As this polymerization is extremely rapid and complete in <1 min even in dilute conditions, a function of % *ee* vs monomer conversion was not determined.

Next, we employed (*S,S*)**-1** to determine its ability to kinetically resolve MMAz. With the slower polymerization rate of MMAz, we were able to analyze several aliquots from a single polymerization reaction and compare the % *ee* values of the unreacted monomer vs % monomer conversion (Figure 6). In the case of MMAz, enantiomeric (*S,S*)**-1** discriminates the enantiomers of the monomer to a greater extent than with MAz, although the kinetic resolution of MMAz is still inefficient (~1.8 *s* values for all aliquots analyzed). Given the stereodifferentiation rendered by a rather small methyl group at the remote $\gamma$ position (in respect to the carbon−carbon double bond) of the monomer, the kinetic resolution of MMAz by the enantiomeric catalyst **1** can be appreciated. It is reasoned that modified monomer structures, inspired by the DFT calculations (vide infra), could lead to a greatly enhanced kinetic resolution of such racemic monomers, which will be a subject of our continued investigation in this area.

Enantioselectivity in the kinetic resolution of MMAz was examined by DFT calculations. We first investigated enantiofacial selectivity in the polymerization of the achiral *N*-methacryloylaziridine. As anticipated, DFT calculations analogous to those performed by some of us to rationalize the enantioselectivity in the polymerization of methyl methacrylate with $C_2$-symmetric metallocenes,[56,57] resulted in a $\Delta E^{\ddagger}_{\text{stereo}}$ of ~3.2 kcal/mol, which is in qualitative agreement with the highly isotactic polymer obtained from the polymerization of MMAz. The most favored transition state was then used to investigate the kinetic resolution of the chiral racemic MMAz by adding a

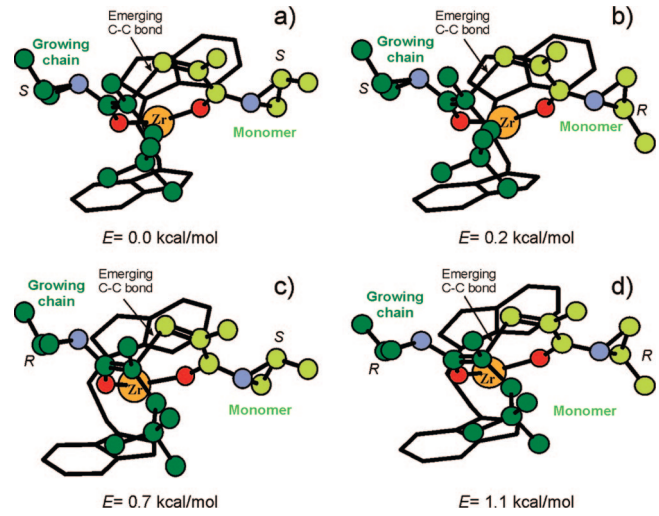


**Figure 7.** Transition states for the kinetic resolution of MMAz by (*S,S*)**-1**. Hydrogen atoms were omitted for clarity.

methyl group on the aziridine ring of both the monomer and the growing chain. Since two stereogenic C centers are generated, we considered four possible transition states corresponding to different combinations of the configuration on the growing chain and on the monomer. These four transition states are defined as *R*-chain/*R*-MMAz if *R* is the configuration of both stereogenic C atoms, *R*-chain/*S*-MMAz if *R* and *S* are the configuration of the stereogenic C atoms on the chain and on the monomer, respectively, and so on. The relative stability of these four transition states is reported in Table 2. In all cases we considered a (*S,S*) coordination of the EBI ligand.

The numbers reported in Table 2 indicate that whatever is the configuration of the stereogenic C atom of the aziridine ring in the growing chain, there is no substantial selectivity in the selection between the two enantiomers of MMAz. In fact, in the case of an *S*-chain, addition of *S*-MMAz is favored by only 0.2 kcal/mol with respect to addition of *R*-MMAz, while in the case of an *R*-chain, addition of *S*-MMAz is favored by only 0.4 kcal/mol with respect to addition of *R*-MMAz. Although the most stable transition state corresponds to addition of *S*-MMAz to an *S*-chain, it is clear that the small energy differences we calculated are in qualitative agreement with the low kinetic resolution obtained experimentally. The structures of the four transition states, depicted in Figure 7, clearly show that in all cases the methyl group on the aziridine ring can be placed quite far away from the EBI ligand as well as from other atoms of the chain and of the monomer, which explains the low efficiency of the kinetic resolution of MMAz.

**Polymerizability of Methacrylamides.** Within two polymerizable methacrylamides (MMAz and MTMAz) investigated so far, the highly strained three-membered aziridine ring built into the methacrylamide monomer structure is believed to render their stable planar conjugated monomer conformations. Natural questions are how the aziridine ring works in this function and can one identify other moieties that function the same way. Successfully addressing these questions will promote rational design of polymerizable methacrylamides and thus substantially expand the polymerizable methacrylamide monomer family.

An apparent design of a planar methacrylamide monomer is to covalently link the α-methyl to one of the methyl groups on N as in the monomer structure of MMPy (Chart 1) which was shown to be radically polymerizable.[73] Another approach is to place sterically bulky, rigid aromatic groups on N for its conjugation with the aromatic ring rather than with the carbonyl group, which could prevent twisting of the C═C bond relative

**Chart 2. Definition of the Torsional Angles $\theta$ and $\omega$ in *N,N*-Dialkylmethacrylamides**

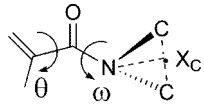


**Table 3. DFT Calculated Torsional Angles and Energies of Amide Enolate Formation**

| monomer | $\theta$ (deg) | $\omega$ (deg) | $E$ (kcal/mol) |
|---|---|---|---|
| DMAA | 6.3 | 59.7 | 22.5 |
| MMAz | 9.7 | 66.5 | 19.6 |
| AMAz | 3.4 | 73.7 | 16.0 |
| MTMAz | 12.9 | 72.4 | 18.5 |
| MMPy | 6.0 | 112.9 | 30.7 |
| DMMA | 131.0 | 46.5 | 25.6 |
| MCBz | 137.7 | 2.6 | 11.0 |

to the C═O bond. To this end, we resided the monomer MCBz (Chart 1). However, neither MMPy nor MCBz was polymerized by **1**, even with extended reaction times (24 h) or elevated temperatures (80 °C). In radical polymerization using AIBN as initiator, MMPy[73] is less reactive than MMAz,[66] which can be explained by the effectiveness of conjugation between the vinyl and carbonyl double bonds, derived from analysis of NMR spectra of monomers as shown by Kodaira et al.[64] Specifically, as effective conjugation in such α,β-unsaturated amide monomers downfield-shifts the vinyl protons rendering the more reactive C═C bond, comparing the vinyl proton $^1$H NMR ($CDCl_3$) chemical shifts in MMPy ($\delta$ 5.81 and 5.19 ppm) vs those in MMAz ($\delta$ 6.09 and 5.63 ppm) suggests poor $\pi$ overlap between the vinyl and carbonyl double bonds in MMPy; this also explains the inactivity of catalyst **1** toward MMPy in that the C═C bond has low reactivity reflected by the upfield-shifted vinyl protons.

Likewise, inspection of the NMR spectra of MCBz provides insight into its nonpolymerizability by catalyst **1**. First, in its $^1$H NMR, the vinyl protons have resonances at 5.69 and 5.63 ppm in $CDCl_3$, as in the case of the nonpolymerizable DMMA ($\delta$ 5.19 and 5.03 ppm), corresponding to the much higher magnetic field than the vinyl protons in the polymerizable MMAz. Second, if there is effective conjugation between the vinyl and carbonyl double bonds, then in the $^{13}$C NMR there shows a small $\Delta\delta$ between the α- and β-carbon chemical shifts. Accordingly, the nonpolymerizable MCBz and DMMA have $\Delta\delta$ of 19.1 and 25.4 ppm, respectively, while the polymerizable MTMAz, MMA, and MMAz have smaller $\Delta\delta$ of 10.7, 10.8, and 15.3 ppm, respectively.

To systematically rationalize the reactivity of the different acrylamides listed in Chart 1, we performed DFT calculations on these monomer molecules. To characterize the assumed geometry, we use the torsional angle $\theta$, defined as the C═C−C═O torsional angle (Chart 2), and the torsional angle $\omega$, defined as the O═C−N−$X_C$ torsional angle, where $X_C$ is the middle point between the two C atoms bonded to the N atom (Chart 2). According to this definition, if the C═C bond and the N atom are conjugated to the C═O bond, then the $\theta$ and $\omega$ dihedral angles should be close to 0° and 90°, respectively.

According to our DFT calculations, DMAA, MMAz, AMAz, MTMAz, and MMPy assume a substantially planar geometry based on their small $\theta$ values (3.4°−12.9°, Table 3), whereas DMMA and MCBz assume a strongly nonplanar geometry, as indicated by their $\theta$ value of 131.0° and 137.7°, respectively. As described in the Introduction, DMMA is forced to assume a nonplanar conformation at both the $\theta$ and $\omega$ angles because of steric repulsion between the methacrylic methyl and one of the N-bonded methyl groups.

**Scheme 3. Hypothetic Reaction Designed To Investigate the Stability of the Amide−Enolate Chain**

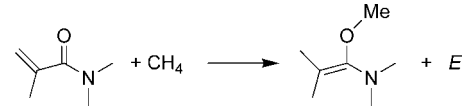


Moving to the $\omega$ angle, we found that with the exception of MCBz, which presents an $\omega$ angle close to 0°, all the monomers present $\omega$ angles deviating considerably from 90° (see Table 3), which indicates somewhat limited conjugation of the N lone pair to the C═O bond. Moreover, in AMAz, MMAz, and MTMAz the geometric constraint of the three-membered aziridine ring forces an almost $sp^3$ hybridization at the N atom, which results in remarkably reduced ring strain[80] but imposes a pyramidal geometry at the N atom. Consequently, the lone pair of the N atom is in a $sp^3$ atomic orbital that geometrically cannot overlap properly with $\pi$ orbitals of the C═O bond in AMAz, MMAz, and MTMAz, suppressing conjugation between the N atom and the C═O bond. However, in terms of monomer geometry the presence of the aziridine ring, as previously noted, pulls the N substituents away from the methacryclic methyl group, allowing for the monomers to assume a planar geometry around the $\theta$ angle. The $\omega$ close to 0° of MCBz, which indicates complete absence of conjugation between the N atom and the C═O bond, can be rationalized considering that the N atom participates to the extended aromatic systems of the N-substituent.

Focusing on the $\theta$ angle, our findings qualitatively correlate with the proposal that nonplanar acrylamides, such as DMMA and MCBz, are nonpolymerizable because of poor overlap between the $\pi$ orbitals of the vinyl C═C and carbonyl C═O bonds. The only exception here is represented by MMPy, which is planar but nonpolymerizable by the current catalyst system. In order to provide further insights into this issue, we also investigated the enolate formation energies that can formally be derived from the hypothetic reaction depicted in Scheme 3 in the case of DMMA. This reaction allows us to investigate the acrylamide to enolate conversion without the steric bulkiness of the (EBI)Zr ligand. The basic idea here is that the amide−enolate is a good model of the amide−enolate chain formed during the polymerization.

The energetic values $E$ of the reaction shown in Scheme 3 are reported also in Table 3. First, all the $E$ values are positive, which means that the amide−enolates are less stable than separated acrylamide and methane. Within this scheme, the smaller is $E$ the easiest is enolate formation and, consequently, polymerization. Indeed, our calculations indicate that the polymerizable DMAA, MMAz, AMAz, and MTMAz monomers exhibit rather smaller $E$ values compared to the nonpolymerizable DMMA and MMPy monomers. The only exception here is represented by MCBz.

The relative stability of the enolate intermediates can be easily rationalized considering that a formal C═C double bond is localized on the internal C−C bond of the monomers. The amide−enolate from DMMA, $E$ = 25.6 kcal/mol, is destabilized by the same steric interactions that impose a nonplanar geometry in the monomer. The amide−enolate from MMPy, $E$ = 30.7 kcal/mol, is destabilized by having the C═C bond moved into the six-membered ring, which introduces higher ring stain. In the DMAA, AMAz, MMAz, and MTMAz derived amide−enolates, $E$ = 16.0−22.5 kcal/mol, the geometric constraint of the three-membered-aziridine ring, as discussed above, prevents the N atom to assume a $sp^2$ planar geometry, so that the N atom is not conjugated to the C═C bond, and no steric interactions between the N substituents and other groups are introduced. MCBz, with a $E$ = 11.0 kcal/mol, presents the only exception.

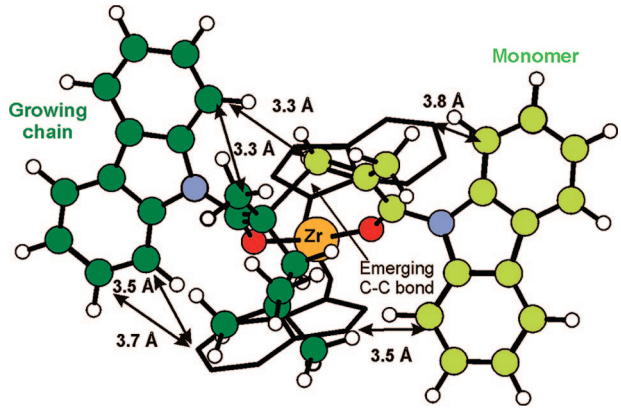


**Figure 8.** Transition state for the Michael addition in MCBz polymerization by **1**.

**Scheme 4. Reaction Used To Estimate Steric Effects in MCBz Polymerization by 1**

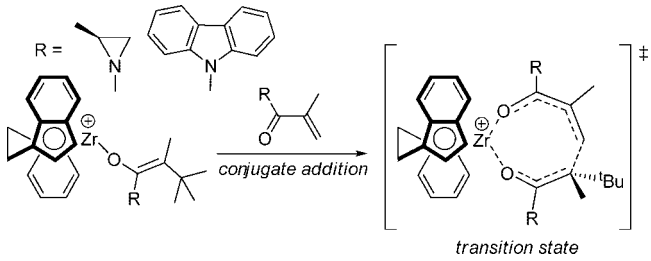


This low *E* value is associated with the participation of the N atom to the extended aromatic systems of the N-substituent. As noted above, this interaction effectively removes participation of N atom of MCBz to the amide bond, which reduces the energy loss in the monomer to enolate transformation. According to this chemical framework, MCBz should be a highly polymerizable monomer. However, MCBz is by far the monomer with the bulkier N group, which suggests that the experimental nonpolymerizability of MCBz could be connected to severe steric repulsion between the bulky aromatic N-substituent and the metallocene skeleton. To investigate better this point, we investigated the transition state of the Michael addition step in the case of MCBz (see Figure 8).

Visual inspection reveals several short distances between atoms of the bulky N-substituent of both the growing chain and the monomer with other atoms. The remarkable steric pressure in the transition state revealed in Figure 8 is also evident by comparison with the stable transition states of MMAz depicted in Figure 7. Energetically, to reach the transition state for Michael addition from separated (EBI)Zr−(amide−enolate) and monomer (Scheme 4) is ∼17 kcal/mol more expensive for MCBz than for MMAz, which is another indication of the highly destabilizing steric interactions in the case of MCBz polymerization.

Concluding this part, our DFT results suggest that DMAA, AMAz, MMAz, and MTMAz are polymerizable monomers toward conjugate addition polymerization due to stability of the resulting amide enolate chain. As for the nonpolymerizable DMMA, MMPy, and MCBz monomers, DMMA is nonpolymerizable because of steric repulsion between the N-substituents and the methyl group in the methacrylic position, MMPy is nonpolymerizable because of ring strain in the amide−enolate growing chain, and MCBz is nonpolymerizable because of steric repulsion between the large N-substituent and the EBI skeleton during the Michael addition step.

## Conclusions

We reported in this contribution the first successful coordination−addition polymerization of *N,N*-dialkylmethacrylamides by metallocene catalysts. The polymerizable methacrylamides investigated in this study are MMAz and MTMAz, both of which incorporate the highly strained three-membered aziridine ring. The geometric constraint of the aziridine ring forces an almost $sp^3$ hybridization at the N atom that adopts a pyramidal geometry and suppresses conjugation between the N atom and the C═O bond, thereby effectively pulling the N-substituents away from the methacryclic methyl group and allowing for the monomers to assume a planar geometry with substantial conjugation between the vinyl and carbonyl double bonds.

The polymerization of MMAz by chiral zirconocenium catalyst **1** is highly stereospecific and exhibits a high degree of control over polymerization. Kinetic studies showed that the methacrylamide polymerization proceeds in the same manner as the acrylamide polymerization by **1**, with intramolecular conjugate addition within the catalyst−monomer complex being the fast step and associative displacement of the coordinated penultimate amide group within the eight-membered-ring amide enolate resting intermediate by incoming monomer to regenerate the catalyst−monomer complex being the rate-determining step.

Excitingly, we demonstrated experimentally and theoretically the capability of enantiomeric catalyst **1** for kinetic resolution of the racemic MMAz monomer. The stereoselectivity factor ($s \sim 1.8$) is currently low but still appreciative, given the small aziridine methyl group at the remote $\gamma$ position (in respect to the C═C bond) of the monomer. On the basis of these results, we reasoned that modified racemic monomer structures such as those incorporating 1,2-disubstituted aziridines could impose much more pronounced stereodifferentiation and thus greatly enhance kinetic resolution of such racemic methacrylamide monomers by the chiral metallocene catalysts. The research directed to this effort is underway.

We also investigated the scope of the polymerizable methacrylamide monomers for two purposes. First, the substituent on the highly strained aziridine ring was explored to module thermally induce cross-linking process occurring through ring-opening of the aziridine ring. To this end, we found that poly(MTMAz) with the cyclic tetramethylene substitution greatly enhance resistance toward thermal cross-linking as marked by an enhancement of 57 °C in onset $T_c$ and 42 °C in maximum $T_c$ over poly(MMAz) with the methyl substitution. Second, pendant moieties other than aziridines were explored to overcome the propensity for *N,N*-disubstituted methacrylamides to assume the twisted confirmation. Although neither of the monomers tested (MMPy and MCBz) derived from two different designs are polymerizable using metallocene catalyst **1**, analysis of their $^1$H and $^{13}$C NMR features and comparing them with the known conjugated polymerizable α,β-unsaturated ester and amide monomers provided insight into their nonpolymerizability or relative reactivity. These studies, combined with DFT calculations on the monomer geometry and relative energy for the formation of amide−enolate intermediates, show that nonpolymerizable methacrylamides either do not exhibit conjugation between the C═C and C═O bonds (e.g., DMMA, MCBz) or have high energy for the amide−enolate formation (e.g., MMPy).

**Acknowledgment.** This work was supported by the National Science Foundation (NSF-0718061) for the work carried out at Colorado State University and INSTM (Cineca Grant Key-Project 2008) for the work carried out at the University of Salerno. We thank Prof. Tom Rovis (CSU) for assistance in % *ee* measurements and Boulder Scientific Co. for the research gift of $B(C_6F_5)_3$.

## References and Notes


(1) Selected recent reference works and reviews: (a) Chen, E. Y.-X.; Rodriguez-Delgado, A. Complexes of Zirconium and Hafnium in Oxidation State IV. In *Comprehensive Organometallic Chemistry III*; Bochmann, M., Vol. Ed.; Mingos, M. P., Crabtree, R. H., Chief Eds.; Elsevier: Oxford, 2007; Vol. *4*, pp 759−1004. (b) Cuenca, T. Complexes of Titanium in Oxidation State IV. In *Comprehensive Organometallic Chemistry III*; Bochmann, M., Vol. Ed.; Mingos, M. P., Crabtree, R. H., Chief Eds.; Elsevier: Oxford, 2007; Vol. *4*, pp 323−696. (c) Bochmann, M. Cationic Group 4 Metallocene Complexes and Their Role in Polymerisation Catalysis: the Chemistry of Well Defined Ziegler Catlaysts. *J. Chem. Soc., Dalton Trans.* **1996**, 255–270. (d) Jordan, R. F. Chemistry of Cationic Dicyclopentadienyl Group 4 Metal-Alkyl Complexes. *Adv. Organomet. Chem.* **1991**, *32*, 325–387.

(2) Selected books, reference works, or journal reviews: (a) *Stereoselective Polymerization with Single-Site Catalysts*; Baugh, L. S., Canich, J. A. M., Eds.; CRC Press: Boca Raton, FL, 2008. (b) Resconi, L.; Chadwick, J. C.; Cavallo, L. Olefin Polymerizations with Group IV Metal Catalysts. In *Comprehensive Organometallic Chemistry III*; Bochmann, M., Vol. Ed.; Mingos, M. P., Crabtree, R. H., Chief Eds.; Elsevier: Oxford, 2007; Vol. *4*, pp 1005−1166. (c) Domski, G. J.; Rose, J. M.; Coates, G. W.; Bolig, A. D.; Brookhart, M. Living Alkene Polymerization: New Methods for the Precision Synthesis of Polyolefins. *Prog. Polym. Sci.* **2007**, *32*, 30–92. (d) Marks, T. J. *Proc. Natl. Acad. Sci. U.S.A.* **2006**, *103*, 15288–15354, and contributions therein (issue on "Polymerization Special Feature"). (e) Gibson, V. C.; Spitzmesser, S. K. Advances in Non-Metallocene Olefin Polymerization Catalysis. *Chem. Rev.* **2003**, *103*, 283–315. (f) Gladysz, J. A. *Chem. Rev.* **2000**, *100*, 1167–1681, and contributions therein (issue on "Frontiers in Metal-Catalyzed Polymerization"). (g) Brintzinger, H. H.; Fischer, D.; Mülhaupt, R.; Rieger, B.; Waymouth, R. M. Stereospecific Olefin Polymerization. *Angew. Chem., Int. Ed.* **1995**, *34*, 1143–1170.

(3) Ning, Y.; Chen, E. Y.-X. *J. Am. Chem. Soc.* **2008**, *130*, 2463–2465.

(4) Mariott, W. R.; Escudé, N. C.; Chen, E. Y.-X. *J. Polym. Sci., Part A: Polym. Chem.* **2007**, *45*, 2581–2592.

(5) Lian, B.; Thomas, C. M.; Navarro, C.; Carpentier, J.-F. *Organometallics* **2007**, *26*, 187–195.

(6) Ning, Y.; Chen, E. Y.-X. *Macromolecules* **2006**, *39*, 7204–7215.

(7) Rodriguez-Delgado, A.; Mariott, W. R.; Chen, E. Y.-X. *J. Organomet. Chem.* **2006**, *691*, 3490–3497.

(8) Rodriguez-Delgado, A.; Chen, E. Y.-X. *Macromolecules* **2005**, *38*, 2587–2594.

(9) Kostakis, K.; Mourmouris, S.; Kotakis, K.; Nikogeorgos, N.; Pitsikalis, M.; Hadjichristidis, N. *J. Polym. Sci., Part A: Polym. Chem.* **2005**, *43*, 3305–3314.

(10) Ning, Y.; Cooney, M. J.; Chen, E. Y.-X. *J. Organomet. Chem.* **2005**, *690*, 6263–6270.

(11) Lian, B.; Lehmann, C. W.; Navarro, C.; Carpentier, J.-F. *Organometallics* **2005**, *24*, 2466–2472.

(12) Bolig, A. D.; Chen, E. Y.-X. *J. Am. Chem. Soc.* **2004**, *126*, 4897–4906.

(13) Stojcevic, G.; Kim, H.; Taylor, N. J.; Marder, T. B.; Collins, S. *Angew. Chem., Int. Ed.* **2004**, *43*, 5523–5526.

(14) Strauch, J. W.; Fauré, J.-L.; Bredeau, S.; Wang, C.; Kehr, G.; Fröhlich, R.; Luftmann, H.; Erker, G. *J. Am. Chem. Soc.* **2004**, *126*, 2089–2104.

(15) Karanikolopoulos, G.; Batis, C.; Pitsikalis, M.; Hadjichristidis, N. *J. Polym. Sci., Part A: Polym. Chem.* **2004**, *42*, 3761–3774.

(16) Ferenz, M.; Bandermann, F.; Sustmann, R.; Sicking, W. *Macromol. Chem. Phys.* **2004**, *205*, 1196–1205.

(17) Rodriguez-Delgado, A.; Mariott, W. R.; Chen, E. Y.-X. *Macromolecules* **2004**, *37*, 3092–3100.

(18) Lian, B.; Toupet, L.; Carpentier, J.-F. *Chem.—Eur. J.* **2004**, *10*, 4301–4307.

(19) Jensen, T. R.; Yoon, S. C.; Dash, A. K.; Luo, L.; Marks, T. J. *J. Am. Chem. Soc.* **2003**, *125*, 14482–14494.

(20) Chen, E. Y.-X.; Cooney, M. J. *J. Am. Chem. Soc.* **2003**, *125*, 7150–7151.

(21) Mariott, W. R.; Chen, E. Y.-X. *J. Am. Chem. Soc.* **2003**, *125*, 15726–15727.

(22) Jin, J.; Mariott, W. R.; Chen, E. Y.-X. *J. Polym. Chem., Part A: Polym. Chem.* **2003**, *41*, 3132–3142.

(23) Batis, C.; Karanikolopoulos, G.; Pitsikalis, M.; Hadjichristidis, N. *Macromolecules* **2003**, *36*, 9763–9774.

(24) Karanikolopoulos, G.; Batis, C.; Pitsikalis, M.; Hadjichristidis, N. *Macromol. Chem. Phys.* **2003**, *204*, 831–840.

(25) Bolig, A. D.; Chen, E. Y.-X. *J. Am. Chem. Soc.* **2002**, *124*, 5612–5613.

(26) Jin, J.; Chen, E. Y.-X. *Organometallics* **2002**, *21*, 13–15.

(27) Jin, J.; Wilson, D. R.; Chen, E. Y.-X. *Chem. Commun.* **2002**, 708–709.

(28) Jin, J.; Chen, E. Y.-X. *Macromol. Chem. Phys.* **2002**, *203*, 2329–2333.

(29) Bandermann, F.; Ferenz, M.; Sustmann, R.; Sicking, W. *Macromol. Symp.* **2001**, *174*, 247–253.

(30) Karanikolopoulos, G.; Batis, C.; Pitsikalis, M.; Hadjichristidis, N. *Macromolecules* **2001**, *34*, 4697–4705.

(31) Bolig, A. D.; Chen, E. Y.-X. *J. Am. Chem. Soc.* **2001**, *123*, 7943–7944.

(32) Frauenrath, H.; Keul, H.; Höcker, H. *Macromolecules* **2001**, *34*, 14–19.

(33) Nguyen, H.; Jarvis, A. P.; Lesley, M. J. G.; Kelly, W. M.; Reddy, S. S.; Taylor, N. J.; Collins, S. *Macromolecules* **2000**, *33*, 1508–1510.

(34) Bandermann, F.; Ferenz, M.; Sustmann, R.; Sicking, W. *Macromol. Symp.* **2000**, *161*, 127–134.

(35) Cameron, P. A.; Gibson, V.; Graham, A. J. *Macromolecules* **2000**, *33*, 4329–4335.

(36) Stuhldreier, T.; Keul, H.; Höcker, H. *Macromol. Rapid Commun.* **2000**, *21*, 1093–1098.

(37) Chen, E. Y.-X.; Metz, M. V.; Li, L.; Stern, C. L.; Marks, T. J. *J. Am. Chem. Soc.* **1998**, *120*, 6287–6305.

(38) Shiono, T.; Saito, T.; Saegusa, N.; Hagihara, H.; Ikeda, T.; Deng, H.; Soga, K. *Macromol. Chem. Phys.* **1998**, *199*, 1573–1579.

(39) Hong, E.; Kim, Y.; Do, Y. *Organometallics* **1998**, *17*, 2933–2935.

(40) Li, Y.; Ward, D. G.; Reddy, S. S.; Collins, S. *Macromolecules* **1997**, *30*, 1875–1883.

(41) Deng, H.; Shiono, T.; Soga, K. *Macromol. Chem. Phys.* **1995**, *196*, 1971–1980.

(42) Deng, H.; Shiono, T.; Soga, K. *Macromolecules* **1995**, *28*, 3067–3073.

(43) Soga, K.; Deng, H.; Yano, T.; Shiono, T. *Macromolecules* **1994**, *27*, 7938–7940.

(44) Collins, S.; Ward, D. G.; Suddaby, K. H. *Macromolecules* **1994**, *27*, 7222–7224.

(45) Collins, S.; Ward, S. G. *J. Am. Chem. Soc.* **1992**, *114*, 5460–5462.

(46) Lian, B.; Thomas, C. M.; Navarro, C.; Carpentier, J.-F. *Macromolecules* **2007**, *40*, 2293–2294.

(47) Mariott, W. R.; Rodriguez-Delgado, A.; Chen, E. Y.-X. *Macromolecules* **2006**, *39*, 1318–1327.

(48) Kostakis, K.; Mourmouris, S.; Pitsikalis, M.; Hadjichristidis, N. *J. Polym. Sci., Part A: Polym. Chem.* **2005**, *43*, 3337–3348.

(49) Deng, H.; Soga, K. *Macromolecules* **1996**, *29*, 1847–1848.

(50) Miyake, G. M.; Chen, E. Y.-X. *Macromolecules* **2008**, *41*, 3405–3416.

(51) Miyake, G. M.; Mariott, W. R.; Chen, E. Y.-X. *J. Am. Chem. Soc.* **2007**, *129*, 6724–6725.

(52) Mariott, W. R.; Chen, E. Y.-X. *Macromolecules* **2005**, *38*, 6822–6832.

(53) Mariott, W. R.; Chen, E. Y.-X. *Macromolecules* **2004**, *37*, 4741–4743.

(54) Spaether, W.; Klaβ, K.; Erker, G.; Zippel, F.; Fröhlich, R. *Chem.—Eur. J.* **1998**, *4*, 1411–1417.

(55) Ning, Y.; Caporaso, L.; Correa, A.; Gustafson, L. O.; Cavallo, L.; Chen, E. Y.-X. *Macromolecules* **2008**, *41*, 6910–6919.

(56) Caporaso, L.; Cavallo, L. *Macromolecules* **2008**, *41*, 3439–3445.

(57) Caporaso, L.; Gracia-Budrìa, J.; Cavallo, L. *J. Am. Chem. Soc.* **2006**, *128*, 16649–16654.

(58) Tomasi, S.; Weiss, H.; Ziegler, T. *Organometallics* **2007**, *26*, 2157–2166.

(59) Tomasi, S.; Weiss, H.; Ziegler, T. *Organometallics* **2006**, *25*, 3619–3630.

(60) Hölscher, M.; Keul, H.; Höcker, H. *Macromolecules* **2002**, *35*, 8194–8202.

(61) Hölscher, M.; Keul, H.; Höcker, H. *Chem.—Eur. J.* **2001**, *7*, 5419–5426.

(62) Sustmann, R.; Sicking, W.; Bandermann, F.; Ferenz, M. *Macromolecules* **1999**, *32*, 4204–4213.

(63) Xie, X.; Hogen-Esch, T. E. *Macromolecules* **1996**, *29*, 1746–1752.

(64) Kodaira, T.; Tanahashi, H.; Hara, K. *Polym. J.* **1990**, *22*, 649–659.

(65) Okamoto, Y.; Yuki, H. *J. Polym. Sci., Polym. Chem. Ed.* **1981**, *19*, 2647–2650.

(66) (a) Suzuki, T.; Kusakabe, J.; Ishizone, T. *Macromolecules* **2008**, *41*, 1929–1936. (b) Suzuki, T.; Kusakabe, J.; Ishizone, T. *Macromol. Symp.* **2007**, *249*−*250*, 412–416.

(67) Christoffers, J.; Schulze, Y.; Pickardt, J. *Tetrahedron* **2001**, *57*, 1765–1769.

(68) (a) Grossman, R. B.; Doyle, R. A.; Buchwald, S. L. *Organometallics* **1991**, *10*, 1501–1505. (b) Collins, S.; Kuntz, B. A.; Taylor, N. J.; Ward, D. G. *J. Organomet. Chem.* **1988**, *342*, 21–29.

(69) Diamond, G. M.; Jordan, R. F.; Petersen, J. L. *J. Am. Chem. Soc.* **1996**, *118*, 8024–8033.

(70) LoCoco, M. D.; Jordan, R. F. *J. Am. Chem. Soc.* **2004**, *126*, 13918–13919.

(71) (a) Carpentier, J.-F.; Maryin, V. P.; Luci, J.; Jordan, R. F. *J. Am. Chem. Soc.* **2001**, *123*, 898–909. (b) Stevens, J. C.; Timmers, F. J.; Wilson,

D. R.; Schmidt, G. F.; Nickias, P. N.; Rosen, R. K.; Knight, G. W.; Lai, S. Eur. Pat. Appl. EP 0 416815 A2, 1991.
(72) Chen, Y.-X.; Marks, T. J. *Organometallics* **1997**, *16*, 3649–3657.
(73) Ueda, M.; Takahashi, M.; Suzuki, T. *J. Polym Sci. Polym. Phys. Ed.* **1983**, *20*, 1139–1149.
(74) (a) ADF**2007**, Users's Manual, *Theoretical Chemistry*; Vrije Universiteit, Amsterdam, **2007**. (b) Baerends, E. J.; Ellis, D. E.; Ros, P. *Chem. Phys.* **1973**, *2*, 41–51.
(75) Vosko, S.-H.; Wilk, L.; Nusair, M. *Can. J. Phys* **1980**, *58*, 1200–1211.
(76) Becke, A. D. *Phys. Rev. A* **1988**, *38*, 3098–3100.
(77) (a) Perdew, J. P. *Phys. Rev. B* **1986**, *33*, 8822–8824. (b) Perdew, J. P. *Phys. Rev. B* **1986**, *34*, 7406–7406.
(78) (a) Klamt, A.; Schüürmann, G. *J. Chem. Soc., Perkin Trans.* **1993**, 799–805. (b) Pye, C. C.; Ziegler, T. *Theor. Chim. Acta* **1999**, *101*, 396–408.
(79) Eliel, A. L.; Wilen, S. H.; Mander, L. N. *Stereochemistry of Organic Compounds*; John Wiley & Sons: New York, 1994; pp 266−268.
(80) The ideal $sp^3$ valence angle of 109.47° is closer to the 60° valence angle of a three-membered ring than the ideal $sp^2$ value of 120°.

MA802697Z